Astron. Astrophys. 330, 232–242 (1998)

ASTRONOMY
AND
ASTROPHYSICS

Inferring acetylene abundances from C_2H: the C_2H_2/HCN abundance ratio

A. Fuente[1], **J. Cernicharo**[2], **and A. Omont**[3]

[1] Observatorio Astronómico Nacional (IGN), Campus Universitario, Apdo. 1143, E-28800 Alcalá de Henares (Madrid), Spain
[2] Consejo Superior de Investigaciones Científicas (CSIC) Serrano 123, E-28006 Madrid, Spain
[3] Institut d'Astrophysique de Paris (CNRS), 98 bis Bd Arago, F-75014 Paris, France

Received 21 March 1997 / Accepted 24 September 1997

Abstract. We have carried out a survey of C_2H and HCN in a wide sample of evolved stars using the 30-m IRAM telescope. Significant variations of the C_2H abundance are found between the observed stars. Low C_2H abundances, X(C_2H)$<10^{-5}$, are observed in S-stars, and detached envelopes. In massive C-rich stars ($\dot{M} > 2\ 10^{-6}\ M_\odot\ \mathrm{yr}^{-1}$) the C_2H abundance seems to be correlated with the expansion velocity. Thus, the mean value of the C_2H abundance is 1.2 10^{-5} in C-rich stars with $V_e \leq 22$ kms^{-1} (hereafter "low-V_e" stars) and a factor of 5 larger, $\sim 5\ 10^{-5}\ M_\odot\ \mathrm{yr}^{-1}$, in those with $V_e \geq 22$ kms^{-1} (hereafter "high-V_e" stars). Some explanations are suggested to account for the large C_2H abundances observed in "high-V_e" stars.

The emission of the HCN lines is optically thick in most C-rich stars. The apparent variations of the HCN abundance with $\dot{M}$ and V_e are very likely due to an opacity effect. The most recent determination, based on ISO data, of the HCN abundance in IRC+10216 is X(HCN) $\sim 3\ 10^{-5}$. From $H^{13}CN$ observations, we have obtained HCN abundances ranging from 3 to 30 10^{-5} in "high-V_e" stars. While HCN abundances $\sim 3\ 10^{-5}$ are found toward AFGL 809 and AFGL 2901 in agreement with the value found in IRC+10216, abundances $\geq 10^{-4}$ are estimated in IRC+00365, IRC+10401, IRC+30374 and S Cep. Based on our C_2H data and assuming X(HCN) $\sim 3\ 10^{-5}$ toward the prototypical star IRC+10216, we estimate a C_2H_2/HCN abundance ratio ~ 1. The C_2H_2/HCN ratio in "high-V_e" stars ranges from ~ 0.08 to 7. The large dispersion found in the HCN abundances toward "high-V_e" stars prevent us from detecting any systematic variation of the C_2H_2/HCN ratio with the expansion velocity in massive C-rich stars. In C-rich stars with low mass-loss rate, the C_2H_2/HCN ratio is a factor of 10 lower than in IRC+10216.

Key words: stars: abundances – circumstellar matter – stars: AGB and post-AGB – radio lines: stars – stars: IRC +10216

Send offprint requests to: A. Fuente

1. Introduction

Circumstellar envelopes (CSEs) of C-rich stars are very rich in molecular species. More than 50 species are found in the envelope of the prototypical C-rich star IRC+10216(CW Leo). Besides simple carbon-bearing molecules (CO, CS, CN, HCN,...), large carbon-chain molecules like cyanopolyynes, $HC_{2n+1}N$ (n=1-5),the hydrocarbon radicals C_nN (n=1-3) and C_nH (n=1-8)), carbenes C_nH_2 (n=3-4), and sulphur and silicon bearing species (SiS, SiO,..) are found in its envelope (Cernicharo 1988, Omont 1992, Bujarrabal et al. 1994, Olofsson 1994, Cernicharo & Guelin 1996a and references therein). These species can be divided into parent and daughter molecules. Parent molecules are formed in thermodynamic equilibrium in the stellar photosphere and are ejected with the outflowing material. When the ejected gas reaches the external layers of the envelope where UV photons can penetrate, parent molecules are dissociated into reactive daughter products that give rise to the outer envelope chemistry.

Acetylene (C_2H_2) is formed in the stellar photosphere and is known to play an essential role in grain condensation and in the outer envelope chemistry of C-rich stars. However, very little is known about its spatial abundance profile. In fact, the C_2H_2 abundance has only been estimated toward IRC+10216 (Keady & Ridgway 1993). This poor information is due to its lack of dipole moment, and consequently of rotational spectrum. Only the high excitation lines arising in the bending and stretching levels can be observed from ground-based telescopes. Based on these infrared lines, a C_2H_2 abundance of 8 10^{-5} has been determined toward IRC+10216 (Keady & Ridgway 1993). Even in this case, the high excitation lines trace mainly the C_2H_2 molecules in the accelerating gas of the inner envelope, and provide very little information about the gas at the terminal expansion velocity of the CSE. The knowledge of the C_2H_2 abundance in the outer envelope is important for two reasons: i) the difference between the C_2H_2 abundance in the photosphere and in the outer envelope constitute an important clue to determine the role of C_2H_2 in grain formation; ii) the determination of the C_2H_2 abundance is essential to understand the formation

of large carbon chains ($HC_{2n+1}N$, C_nH, C_nH_2) in C-rich stars. Theoretically, the only way to determine the C_2H_2 abundance in the outer envelope is indirectly by estimating the C_2H abundance. C_2H is the photodissociation product of acetylene and chemical models predict a quite uniform C_2H/C_2H_2 abundance ratio for the conditions prevailing in C-rich envelopes (Cherchneff et al. 1993, Millar & Herbst 1994). However, although C_2H was detected in evolved stars several years ago (Truong-Bach et al. 1987), there has not been a systematic survey of this molecule in evolved stars. C_2H abundance estimates have been reported only for IRC+10216 (Truong-Bach et al. 1987, Bieging & Rieu 1988) and the southern C-rich star IRAS15194-5115 (Nyman et al. 1993). In order to determine the C_2H abundance, and indirectly that of C_2H_2, we have carried out a survey of C_2H in evolved stars. We observe significant variations of the C_2H abundance with mass loss rate and expansion velocity in C-rich stars. In particular, we detect a group of C-rich stars characterized by having large mass loss rates and large expansion velocities, "high-V_e" stars, in which the C_2H abundance is a factor of 5 larger than in the rest of C- stars.

Another parent molecule whose abundance is essential to understand the chemistry of circumstellar envelopes is HCN. This molecule has been extensively observed in the J=1→0 rotational line, but the higher rotational lines have not been so widely studied. We present a survey of the HCN 2→1 and 3→2 lines toward 19 C-rich stars. Six of these stars, the "high-V_e" stars, were also observed in the HCN 1→0 and $H^{13}CN$ 1→0 line. Our data show that the HCN abundance estimates made using the J=1→0 line could be strongly affected by opacity effects, which are so large, that mask the possible variations of the HCN abundance from one star to another. Based on our $H^{13}CN$ data we give an estimate of the C_2H_2/HCN abundance ratio in "high-V_e" stars.

2. Observations

2.1. Selected sample of stars

We have observed in C_2H a sample of 35 evolved stars, 33 C-rich stars and two S stars. Nineteen C-rich stars have also been observed in HCN. The coordinates and spectral types of these stars are listed in Table 1. We have divided our sample in C-rich stars, non-standard C-rich stars and the group we call "other objects" which contains pre-planetary nebulae (PPNe) and stars with detached envelopes. In the group of non-standard C-rich stars we only include Y CVn and UU Aur. Y CVn is a J-type star and UU Aur is known to present maser emission in the HCN J=1→0 and the CN N=2→1 lines of the ground vibrational state.

2.2. Description of the observations

Observations of C_2H were carried out during July and December, 1993 using the 30-m telescope. The telescope parameters at the observed frequencies and typical system temperatures are given in Table 2. Pointing was checked before observing each star with a strong continuum source, and the rms of pointing errors is ∼ 2". The N=1→0, N=2→1 and N=3→2 rotational lines of C_2H were observed simultaneously. The spectrometers used were two 512×1 MHz filterbanks (for the 1→0 and 3→2 lines) and an acusto-optical spectrometer with a bandwidth and frequency resolution of 500 MHz and 584 kHz respectively. Each spectrometer were centered to allow the observation of all the hyperfine components of each rotational line simultaneously (see Section 3.1 for further explanation). Differences in calibration between both observing periods were less than 20% for most stars. Only in two sources, CIT-6 and V Cyg, the discrepancies between the spectra taken in both observing runs were larger. In these cases, we have chosen the most intense spectrum as the correct one. Since the telescope beam is ∼ 10" at the frequency of the C_2H N=3→2 line, pointing errors of ∼

Table 1. List of objects

Object	R.A. (1950) (^{h},^{m},^{s})	Dec (1950) (°,',")	d (pc)	$\dot{M}$ ($M_\odot$/year)	V_e (kms^{-1})
C-rich stars					
AFGL 190	01:14:26.3	66:58:08	2290	$1.8\ 10^{-5}$	18.2
IRC+50096	03:22:59.1	47:21:22	620	$3.5\ 10^{-6}$	15.4
AFGL 809	05:40:33.3	32:40:49	1500	$1.5\ 10^{-5}$	28.0
AFGL 865	06:01:17.4	07:26:06	1700	$1.5\ 10^{-5}$	16.0
AFGL 5196	06:26:51.1	08:49:19	2620	$9.5\ 10^{-6}$	33.0
IRC+10216	09:45:14.8	13:30:41	200	$2.0\ 10^{-5}$	15.0
CIT-6	10:13:11.0	30:49:17	450	$7.0\ 10^{-6}$	17.0
IRC-10236	10:14:34.4	-14:24:31	950	$4.0\ 10^{-6}$	11.0
U Hya	10:35:05.0	-13:07:26	350	$5.0\ 10^{-7}$	8.8
V Hya	10:49:11.3	-20:59:05	330	$2.5\ 10^{-6}$	19.0
IRC+20370	18:39:41.6	17:38:16	700	$8.0\ 10^{-6}$	14.0
IRC+00365	18:39:48.3	-02:20:24	910	$1.3\ 10^{-5}$	35.3
IRC+10401	19:00:53.0	07:26:19	670	$5.3\ 10^{-6}$	25.0
AFGL 2333	19:07:34.0	09:21:56	1880	$3.3\ 10^{-5}$	19.0
V Aql	19:01:43.9	-05:45:38	350	$3.4\ 10^{-7}$	9.2
IRC-10502	19:17:35.3	-08:07:49	750	$6.2\ 10^{-6}$	29.1
IRC+30374	19:32:08.8	27:57:30	790	$6.7\ 10^{-6}$	25.7
V Cyg	20:39:41.2	47:57:46	500	$4.0\ 10^{-6}$	13.0
AFGL 2686	20:56:59.8	27:14:59	1050	$5.7\ 10^{-6}$	23.5
S Cep	21:35:52.6	78:23:59	400	$2.5\ 10^{-6}$	25.0
AFGL 2901	22:24:08.1	60:05:25	1200	$1.5\ 10^{-5}$	34.2
AFGL 3068	23:16:42.4	16:55:10	1000	$2.0\ 10^{-5}$	14.0
IRC+40540	23:32:01.3	43:16:27	700	$1.0\ 10^{-5}$	15.0
Non-standard C-rich stars					
UU Aur	06:33:06.6	38:29:16	300	$3.0\ 10^{-7}$	13.0
Y Cvn	12:42:47.1	45:42:48	400	$2.0\ 10^{-7}$	8.0
S stars					
W Aql	19:12:41.8	-07:08:08	450	$1.0\ 10^{-6}$	19.0
Chi Cyg	19:48:38.4	32:47:10	150	$5.0\ 10^{-7}$	9.0
Detached, PPN,...					
R Scl	01:24:40.0	-32:48:07	2300	$1.8\ 10^{-5}$	18.2
U Cam	03:37:29.1	62:29:19	500	$2.0\ 10^{-6}$	21.0
S Sct	18:47:37.1	-07:57:59	620	$5.4\ 10^{-6}$	17.3
TT Cyg	19:39:01.9	32:30:02	960	$2.0\ 10^{-6}$	13.3
AFGL 618	04:39:33.8	36:01:15	1700	$1.0\ 10^{-4}$	19.0
AFGL 2688	21:00:19.9	36:29:45	1500	$1.0\ 10^{-4}$	19.0
SAO 34504	22:27:13.4	54:35:44	2350	$5.0\ 10^{-5}$	10.6

Table 2. Antenna-related parameters

Molecule	Line	Frequency (GHz)	HPBW (")	η_{MB}	η_{ff}	T_{sys} (K)
$H^{13}CN$	1→0	86.340188	27	0.75	0.92	250-500
C_2H^*	1→0	87.316922	"	"	"	"
HCN^*	1→0	88.631852	"	"	"	"
C_2H^*	2→1	174.663219	15	0.50	0.90	1200
HCN	2→1	177.261109	"	"	"	2000
C_2H^*	3→2	262.004266	"	0.35	"	1200
HCN	3→2	265.886438	"	"	"	1500

* Frequency at which the spectrometer was centered.

5" could produce these discrepancies in the line intensity. In Table 3 we present the observational parameters of the C_2H lines. Spectra of the C_2H 1→0, 2→1 and 3→2 lines are shown in Fig. 1.

Observations of the HCN J=1→0, J=2→1 and J=3→2 rotational lines toward the stars AFGL 809, IRC+00365, IRC+10401, IRC+30374, S Cep and AFGL 2901 were carried out in December 1993. A wider sample of stars were observed in HCN J=2→1 and J=3→2 lines in previous observing runs (April 1989 and January 1991). For the stars observed in several observing periods the differences in calibration are less than 10%. However, as we will comment in the following section, the observations of HCN J=2→1 at 177260 MHz are extremely difficult. Calibration errors could be as large as 50% due to the large atmospheric opacities at this frequency. The HCN observational results are also given in Table 3. For the stars not observed in the HCN 1→0 line, we have adopted the most recent HCN 1→0 integrated intensity values found in the literature (references are given in Table 3).

Table 3. Observational parameters (K kms^{-1})*

Object	C_2H			HCN			
	1→0	2→1	3→2	1→0	2→1	3→2	Ref[1]
C-rich							
AFGL 190	3.8	-0.11	-0.12	10			(1)
IRC+50096	-0.02	11.2	27.8	20	50.3	115	(2)
AFGL 809	17.5	10.4	20.7	26.6	27.0	56.7	this work
AFGL 865	6.7	21.7	12.1	7.4	17.2	23.3	(2)
AFGL 5196	-0.02	-0.05	-0.08				
IRC+10216	80.6	248.9	246.8	431			(3)
CIT-6	17.5	33.0	81.6	85.4	125.7	126.7	(3)
IRC-10236	-0.02	-0.04	5.3	3.9	21.3	30.3	(2)
U Hya	-0.01	-0.08	-0.09		-0.45	20.8	
V Hya	-0.02	-0.05	-0.08	6.0	-0.39	16.5	(3)
IRC+20370	-0.02	-0.09	19.6	12.8			(3)
IRC+00365	5.5	30.8	39.4	73.0	63.1	194.2	this work
IRC+10401	19.8	86.1	137.8	45.3	43.2	37.1	this work
AFGL 2333	5.8	5.2	6.8				
V Aql	-0.03	-0.17	-0.19	6.2			(4)
IRC-10502	-0.03	-0.07	-0.11				
IRC+30374	-0.03	-0.15	50.2	22.3	72.2	135.0	this work
V Cyg	-0.02	13.4	36.1	20.9	54.0	101.0	(3)
AFGL 2686	-0.02	-0.06	-0.09	18.8			(2)
S Cep	-0.02	-0.14	25.1	35.8	48.6	68.3	this work
AFGL 2901	12.7	36.5	17.8	27.7	26.9		this work
AFGL 3068	10.2	18.7	-0.19	31.8	-0.43		(3)
IRC+40540	8.2	15.6	0.7	27.7	21.5		(3)
Non-standard C-rich stars							
UU Aur	-0.02	-0.08	-0.09	21.6	4.3	13.5	(2)
Y Cvn	-0.03	-0.15	-0.19	25.4	34.2	45.0	(2)
S stars							
W Aql	-0.02	-0.06	-0.08	18.6			(3)
Chi Cyg	-0.03	-0.13	-0.17	23.1			(3)
Detached, PPN,...							
R Scl	-0.03	-0.11	-0.12	9.8			(2)
U Cam	-0.02	-0.05	5.8	16.8	-0.26	38.3	(2)
S Sct	-0.03	-0.13	-0.2				
TT Cyg	-0.02	-0.06	-0.08				
AFGL 618	6.6	22.8	33.2	30			(3)
AFGL 2688	40.1	64.0	52.4	178.9	130.3		(3)
SAO 34504	4.1	12.9	13.9	16.5			(1)

* Negative numbers correspond to non-detections. The absolute value is the rms of the spectrum.

[1] References for the HCN (1→0) data. Ref: (1) Loup et al. (1993); (2) Lucas et al. (1988); (3) Bujarrabal et al. (1994); (4) Heske et al. (1989).

3. Fractional abundance estimates

We have estimated fractional abundances assuming optically thin emission and a constant rotational temperature and molecular abundance over the emitting region. With these assumptions the fractional abundance is given by

$$f = \frac{3kWV_eB^2D^2}{32ln2\pi^2S\mu^2\dot{N}\Delta R} Z(T_{\rm rot}) \exp(E_{\rm u}/kT_{\rm rot}) \quad (1)$$

where W is the velocity integrated intensity of the line (T_{MB} units), V_e is the expansion velocity, B is the HPBW in radians, D is the distance to the star, S is the line strength, μ is the dipole moment, ν is the frequency, and $\dot{N}$ is the mass loss rate in molecules (H_2 and He) s^{-1}. ΔR is $r_e - r_i$, where r_e and r_i are the external and internal emission radii respectively. This expression assumes also that the angle subtended by the source is smaller than the beam. In the case of IRC+10216 for which r_e is larger than $BD/2$, we adopt the latter as external radius. For most stars, expansion velocities, mass loss rates and distances have been taken from Loup et al. (1993) and Bujarrabal et al. (1994). The adopted values are given in Table 1. For IRC+10401, our molecular observations reveal that the expansion velocity is $\sim$ 25 kms^{-1} rather than 18.2 kms^{-1} that is the value reported by Loup et al. (1993). We have adopted 25 kms^{-1} as the expansion velocity and corrected the mass loss rate accordingly ($\dot{M} \propto V_e^2$).

3.1. C_2H

To estimate the external and internal radii of the C_2H emission we have used the procedure described by Huggins & Glassgold (1982) and Olofsson et al. (1993). This procedure assumes that the C_2H is formed only by the acetylene photodissociation, and is destroyed by photodissociation. The adopted photodissociation rates are $G_o = 3.2\ 10^{-9}$ and $5.1\ 10^{-10}$ s^{-1} for C_2H_2 and C_2H respectively (van Dishoeck 1988). The shielding radius depends on $\dot{M}_d/V_d$, where $\dot{M}_d$ and V_d are the dust mass loss rate and the dust expansion velocity respectively. This parameter has been derived from the 60 μm IRAS flux and the data listed in Table 1 using the expression reported by Olofsson et al. (1993). When the calculated internal radius is $\leq 10^{15}$ cm, we have adopted r_i = 10^{15} cm.

Excitation temperatures have been estimated for the stars in which at least two C_2H rotational lines are detected. Most stars present similar excitation temperature with a mean value of T_{ex} = 8.3 K. However there are some stars with high excitation temperatures. IRC+50096 and V Cyg have excitation temperatures $\sim$ 20 K; for IRC-10236, U Cam, and S Cep, $T_{ex} \gg 10$ K; and an extraordinary high temperature, $T_{ex} > 50$ K, is found for IRC+30374. We consider that this value is very likely due to an anomalous excitation and cannot be used for our abundance estimates. Therefore, we have assumed a constant rotational temperature of 10 K for all the stars, except for IRC+50096, V Cyg, IRC-10236, U Cam, S Cep and IRC+30374 in which we have assumed a rotational temperature of 20 K. The estimated radii, excitation temperatures and the derived C_2H fractional abundances are shown in Table 4.

Table 4 shows that the high excitation temperatures correspond to stars with low mass loss rates. In these stars, the C_2H molecules are expected to be located closer to the star (see r_i in Table 4) and consequently, higher excitation temperatures are expected. This situation is similar to that found for CN by Bachiller et al. (1997). Furthermore, the high C_2H excitation temperature found in IRC+30374 suggests that at least this star could present anomalous excitation. The excitation of C_2H is very complex, and infrared and optical pumping via electronic and vibrational transitions must be taken into account. In particular, infrared pumping via the vibrational transition at 5.4 μm, and the electronic $^2\pi \rightarrow ^2\Sigma$ transition at 2.8 μm could play an important role in the excitation of C_2H. To investigate this effect we have represented the C_2H abundance estimates against the flux of the star at 4 μm (see Fig. 2). There is no correlation between the flux of the star at 4 μm and the derived C_2H abundances. We consider that the overall variations found in C_2H abundances are not produced by the infrared excitation of C_2H, although this effect could be very important in some particular stars. This is consistent with the low excitation temperatures, $T_{ex} \sim 8$ K, found in most C-rich stars.

The most restrictive assumption in our calculations is that the emission is optically thin. C_2H is a $^2\Sigma$ molecule. Each rotational level, N, is split into two fine components with J=N+1/2, N-1/2. Besides, each fine level is split into two hyperfine levels (F=J+1/2, J-1/2) due to the nuclear spin of the hydrogen atom. For this reason the N=1$\rightarrow$0 line is split into 6 hyperfine components that are grouped in two fine structure groups (see Fig. 1). We can estimate the opacity of the C_2H N=1$\rightarrow$0 line using the hyperfine line intensity ratios. Assuming that the excitation temperature is the same for all the hyperfine lines, the integrated intensity ratio between the two intense fine groups is 2 in the optically thin case and $\sim$ 1 in the optically thick limit. The mean value of this ratio toward the stars in which C_2H has been detected is 2 with a maximum deviation of 0.4, proving that the C_2H N=1$\rightarrow$0 line is not very optically thick in our sample.

3.2. HCN

HCN, like C_2H_2, is formed in the inner envelope. At a given radius, the HCN molecules are photodissociated into CN, and the HCN abundance decreases sharply. Then, HCN is distributed in a sphere of radius r centered in the star. For our calculations we have adopted as r the internal radius of the C_2H emission calculated as explained in Section 3.1. The HCN excitation temperatures have been derived from the data shown in Table 3. The derived mean value, T_{ex} = 6 K, and the 1$\rightarrow$0 intensities have been adopted for our abundance estimates. The results are given in Table 4. Since opacity effects are not negligible in HCN, T_{ex} = 6 K is a lower limit to the actual value of the excitation temperature, and reflects the excitation of the outermost layers of the emitting region. Given the simplicity of our calculations, the assumption of a higher excitation temperature would mean to multiply all our estimates by a constant factor (a factor of $\sim$ 2 if T_{ex}=20 K). We would like to point out that there are 3 stars, U Hya, V Hya and U Cam that have been detected in the HCN 3$\rightarrow$2 line but not in the HCN 2$\rightarrow$1 line. V Hya and U Cam have also been detected in the HCN 1$\rightarrow$0 line. Since the observations of the HCN 2$\rightarrow$1 line are extremely difficult (see Section 2.2), we are not going to study this effect in detail. But it is interesting to comment that this apparently "strange" excitation has been observed toward a detached envelope (U Cam) and two C-rich stars with very low $\dot{M}$ (U Hya, V Hya). Strange line ratios can be found in a detached envelope (see Olofsson et al. 1996), and anomalous excitation due to infrared and/or optical pumping is more frequently detected in stars with low $\dot{M}$.

4. C_2H abundances

The mean value of the C_2H fractional abundance is $2.5\ 10^{-5}$ toward C-rich stars (mean value calculated taking into account only detections). However, while at least 7 stars have C_2H abundances $< 10^{-5}$, there are some stars with $X(C_2H) \gtrsim 10^{-4}$ (AFGL 809, IRC+10401 and AFGL 2901). Lower C_2H abundances are measured toward stars with detached envelopes. In fact, U Cam is the only one detected in C_2H, with a fractional abundance of $3.6\ 10^{-6}$. We have not detected C_2H toward any S star with an upper limit $X(C_2H) \leq 10^{-5}$. The three PPNe of our sample have been detected in C_2H with a fractional abundance $< 10^{-5}$. Therefore, it seems that the largest C_2H abundances are associated with "standard" C-rich stars but large differences are found from one star to another.

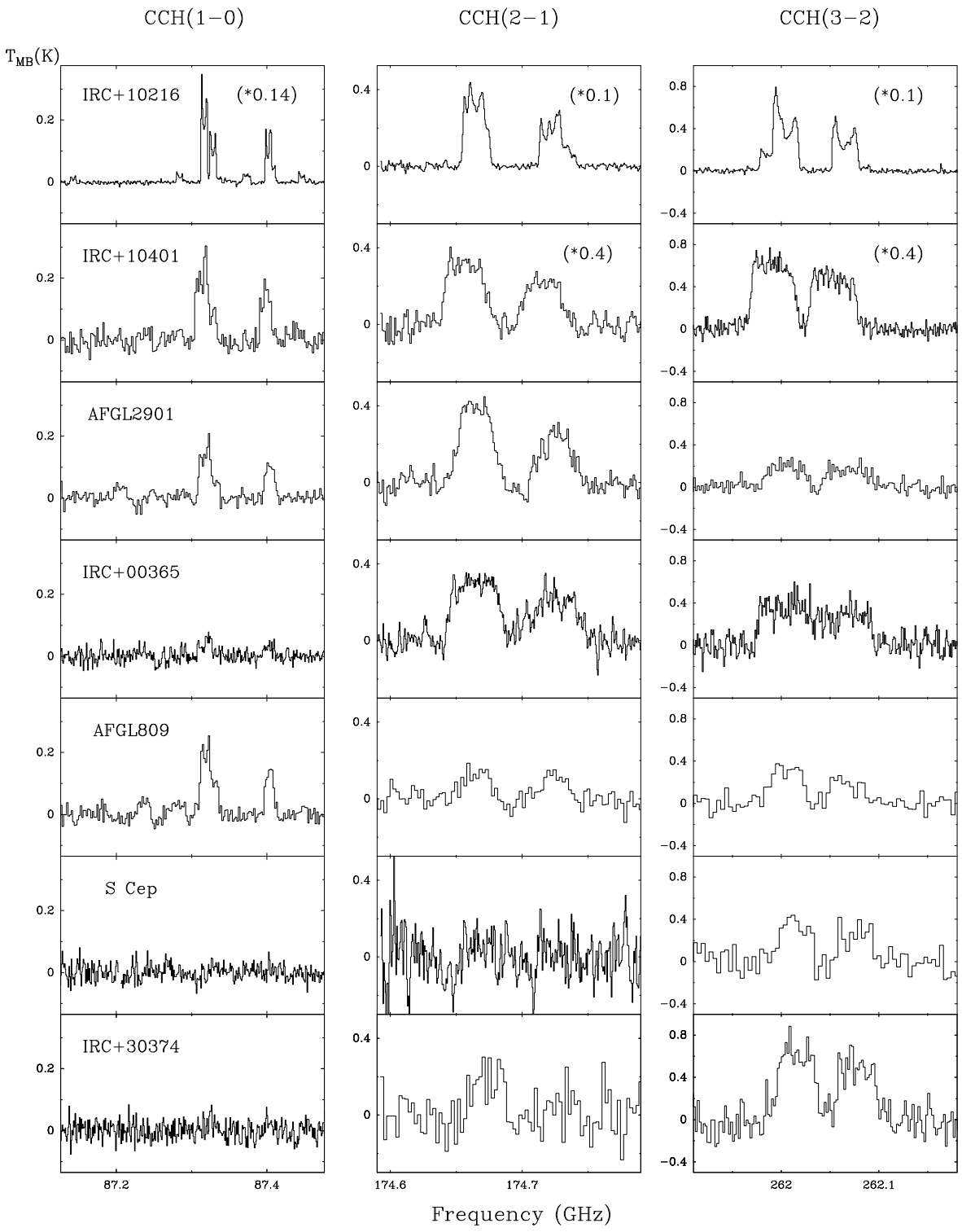

Fig. 1. Spectra of the C_2H N=1→0, 2→1, and 3→2 lines toward the "high-V_e" massive stars. For comparison, we have also included the spectrum toward the prototypical star IRC+10216.

Table 4. Fractional abundances

Object	r_i (10^{16})	r_e (10^{16})	T_{ex}(C_2H) (K)	X_{C_2H}[1]	$T_{ex}(HCN)$	X_{HCN}[2]
C-rich stars						
AFGL 190	2.6	5.4	$\leq$5	2.0 10^{-5}		2.8 10^{-6}
IRC+50096	0.2	1.0	18	1.2 10^{-5}	9	2.3 10^{-5}
AFGL 809	0.8	2.8	6	1.0 10^{-4}	6	1.5 10^{-5}
						* 3.4 10^{-5}
AFGL 865	1.4	3.4	6	2.8 10^{-5}	7	2.2 10^{-6}
AFGL 5196	0.6	2.4		$<$ 7.7 10^{-5}		
IRC+10216	3.4	6.3		1.0 10^{-5}		5.2 10^{-7}
CIT-6	0.5	1.7	8	2.0 10^{-5}	6	1.2 10^{-5}
IRC-10236	0.4	1.4	$\geq$17	2.5 10^{-6}	10	3.3 10^{-6}
U Hya	0.1	0.4		$<$ 1.1 10^{-5}		3.3 10^{-5}
V Hya	0.2	1.0		$<$ 4.6 10^{-6}		3.4 10^{-6}
IRC+20370	0.3	1.2		6.3 10^{-6}		5.0 10^{-6}
IRC+00365	0.6	2.5	9	1.8 10^{-5}	7	3.8 10^{-5}
						*1.0 10^{-4}
IRC+10401	0.3	1.4	9	1.0 10^{-4}	5	9.1 10^{-5}
						*2.9 10^{-4}
AFGL 2333	1.6	4.0	5	1.3 10^{-5}		
V Aql	0.1	0.7		$<$ 2.6 10^{-5}		2.8 10^{-5}
IRC-10502	0.4	1.4		$<$ 2.2 10^{-5}		
IRC+30374	0.3	1.6	$>$50	1.8 10^{-5}	9	2.4 10^{-5}
						*1.3 10^{-4}
V Cyg	0.2	0.8	20	9.4 10^{-6}	8	1.2 10^{-5}
AFGL 2686	0.4	1.8		$<$ 1.5 10^{-5}		2.9 10^{-5}
S Cep	0.1	1.0	$>$15	8.6 10^{-6}	6	7.9 10^{-5}
						*2.8 10^{-4}
AFGL 2901	0.5	2.3	5	6.3 10^{-5}	3	2.1 10^{-5}
						*3.8 10^{-5}
AFGL 3068	1.8	4.0	4	9.3 10^{-6}		1.7 10^{-6}
IRC+40540	0.5	1.7	3	1.4 10^{-5}	3	5.6 10^{-6}
Non-standard C-rich stars						
UU Aur	0.2	0.7		$<$ 2.9 10^{-5}	5	5.8 10^{-5}
Y Cvn	0.1	0.4		$<$ 8.0 10^{-5}	6	2.2 10^{-4}
S stars						
W Aql	0.3	1.3		$<$ 1.7 10^{-5}		3.3 10^{-5}
Chi Cyg	0.1	0.4		$<$ 6.2 10^{-6}		1.3 10^{-5}
Detached, PPN,...						
R Scl	0.2	1.0		$<$ 5.3 10^{-5}		4.3 10^{-6}
U Cam	0.1	0.9	$\geq$11	3.6 10^{-6}		6.1 10^{-5}
S Sct	0.1	0.7		$<$ 1.3 10^{-5}		
TT Cyg	0.1	0.6		$<$ 4.6 10^{-5}		
AFGL 618	14	19	6	2.0 10^{-6}		1.6 10^{-7}
AFGL 2688	14[1]	19[1]	6	9.3 10^{-6}	3	7.5 10^{-7}
SAO 34504	4.3	6.9	7	5.0 10^{-6}		6.2 10^{-7}

[1] Assuming T_{ex}=10 K for all the stars except for IRC+50096, V Cyg, IRC-10236, U Cam, S Cep and IRC+30374 for which T_{ex}=20K.
[2] Assuming T_{ex}=6K for all the stars.
* Estimated assuming $H^{12}CN/H^{13}CN$ = 40.

In Fig. 3 we plot the C_2H abundance against the mass loss rate. We have not detected C_2H toward stars with $\dot{M} \leq$ 2 10^{-6} $M_\odot$ yr^{-1}. The S stars and stars with detached envelopes of our sample have $\dot{M} \leq$ 2 10^{-6} $M_\odot$ yr^{-1}. Since the C/O ratio is lower in S stars than in C-rich stars, carbon-bearing molecules are expected to be less abundant in S stars. Detached envelopes are known to present very peculiar chemistries depending on their evolutionary stage (see Olofsson et al. 1996). Between the "standard" carbon stars with $\dot{M} \leq$ 2 10^{-6} $M_\odot$ yr^{-1}, only toward V Hya we have a significant upper limit to the C_2H abundance (the derived C_2H abundance is at least a factor of 5 lower than the mean value in C-rich envelopes). But the case of V Hya is known to be peculiar with probably a bipolar structure and low molecular abundances (Bujarrabal et al. 1994). Low

C_2H abundances are also derived for the PPNe, SAO34504, AFGL 2688 and AFGL 618, which have mass loss rates ≥ 2 10^{-5} $M_\odot$ yr^{-1}. Such PPNe are surrounded by thick and cool envelopes. In these cases, moderate opacities could very likely produce an underestimate of the C_2H abundance ($\tau \propto \dot{M}$).

The largest C_2H abundances are measured for stars with mass loss rates of $\sim 10^{-5}$ $M_\odot$ yr^{-1}, with typical values X(C_2H) ~ 2 10^{-5} (see Fig. 3). But even if we restrict ourselves to C-rich stars with mass loss rates around 10^{-5} $M_\odot$ yr^{-1}, we find an important dispersion in the values of the C_2H abundance, that ranges from 2.5 10^{-6} (IRC-10236) to 10^{-4} (AFGL 809 and IRC+10401). The three stars with largest C_2H abundances, AFGL 809, IRC+10401 and AFGL 2901, are stars with mass loss rates around 10^{-5} $M_\odot$ yr^{-1}and very large expansion velocities, 28, 25 and 34.2 kms^{-1} respectively. This suggests a possible relationship between the expansion velocity and the C_2H abundance. In Fig. 4 we show the estimated C_2H abundances as a function of the expansion velocity. We have distinguished two different groups of stars, those with expansion velocities ≥ 22 kms^{-1} and those with velocities < 22 kms^{-1}. The mean C_2H abundance in stars with expansion velocities ≥ 22 kms^{-1} is 5.0 10^{-5}, while in stars with expansion velocities < 22 kms^{-1} is 1.2 10^{-5}, i.e., the C_2H abundance is a factor of 5 larger in stars with expansion velocities ≥ 22 kms^{-1} than in stars with expansion velocities < 22 kms^{-1} (these mean values have been calulated taking into account only detections). Within the group of stars with expansion velocities ≥ 22 kms^{-1}, C_2H has not been detected toward AFGL5196, IRC-10502 and AFGL2686. We have not obtained a significant upper limit to the C_2H abundance in AFGL5196. For the two others, the upper limits are 1.2 and 1.5 10^{-5} respectively. In S Cep, the derived C_2H abundance is ~ 9 10^{-6}. The mass loss rate of S Cep is 2.5 10^{-6} $M_\odot$ yr^{-1}, i.e., just in the border between the region of detected and non-detected stars in Fig. 3. It is interesting to point out that within the group of stars with expansion velocities ≥ 22 kms^{-1}, the stars in which we have not detected C_2H as well as S Cep have $\dot{M} < 10^{-5}$ $M_\odot$ yr^{-1}.

In summary, we conclude that the C_2H abundance ranges from a few 10^{-6} to 10^{-4}, and C_2H seems to be underabundant (X(C_2H) $< 10^{-5}$) in S stars and detached envelopes. Values of X(C_2H)$\geq 10^{-5}$ are typically found for C-rich stars with $\dot{M} \gtrsim 10^{-5}$ $M_\odot$ yr^{-1}. Within this group of massive C-rich envelopes, the largest values of the C_2H abundance are found for the stars with $V_e \geq 22$ kms^{-1}, with a mean C_2H abundance ~ 5 10^{-5}. Hereafter, we will refer to the stars with $\dot{M} \gtrsim 10^{-5}$ $M_\odot$ yr^{-1}and $V_e \geq 22$ kms^{-1} as "high-V_e" stars, and to the stars with $\dot{M} \gtrsim 10^{-5}$ $M_\odot$ yr^{-1}and $V_e < 22$ kms^{-1} as "low-V_e" stars.

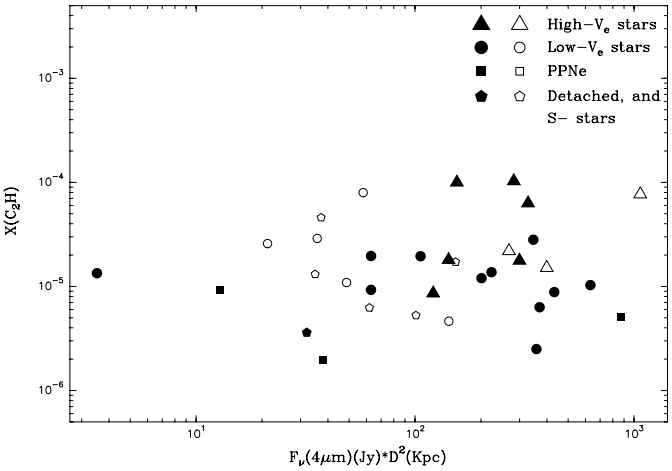

Fig. 2. C_2H abundance estimates against the infrared flux at 4 μm. PPNe are marked with squares, detached envelopes and S stars with pentagons, "high-V_e" massive stars with triangles, and circles represent the rest of C-rich stars. Filled symbols mean detections and empty symbols are upper limits.

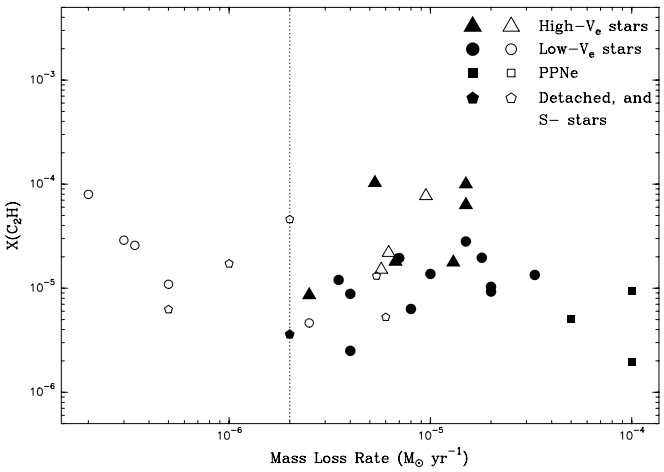

Fig. 3. C_2H abundance estimates against the mass loss rate. Symbols are the same as in Fig. 2. A dashed line is drawn at a mass loss rate of 2 10^{-6} $M_\odot$ yr^{-1}. There is no detection of C_2H for $\dot{M} < 2$ 10^{-6} $M_\odot$ yr^{-1}.

5. HCN abundances

The HCN 1→0 line is very likely optically thick in all the stars of our sample. To study the influence of the opacity in the HCN abundance estimates, we represent in Fig. 5 the abundance estimates against the mass loss rate. The abundances reported by Olofsson et al. (1993) for stars with low mass loss rate are also included in Fig. 5. The HCN abundance apparently decreases with increasing mass loss rate. This is the expected behavior if the emission is optically thick. However, there are some stars with $\dot{M}\sim 10^{-5}$ $M_\odot$ yr^{-1}that seem to have larger HCN abundances (the small shoulder at $\dot{M}\sim 10^{-5}$ $M_\odot$ yr^{-1}in Fig. 5). These stars coincide with those we have previously called "high-V_e" stars and that are characterized by their large expansion velocities.

Jura (1991) suggested that the HCN abundance increases with expansion velocity. However, Olofsson et al. (1993) from a different sample of stars did not find this behavior, but just the opposite. In Fig. 6 we have represented our abundance estimates (we have many stars in common with Jura, 1991) and those of Olofsson et al. (1993), against the expansion velocity. A com-

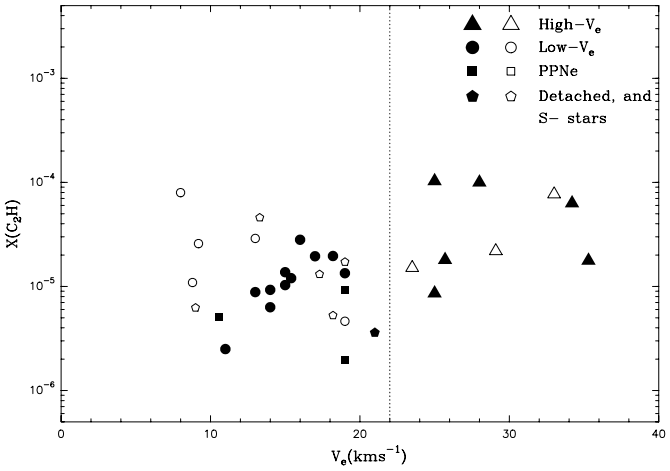

Fig. 4. C_2H abundance estimates against the expansion velocity. Symbols are the same as in Fig. 2 and 3. A dashed line is drawn at a expansion velocity of 22 kms^{-1}. The three non-detections in stars with expansion velocities larger than 22 kms^{-1} correspond to C-rich with $\dot{M} < 10^{-5}$ $M_\odot$ yr^{-1}(AFGL 2686, IRC-10502, AFGL 5196)

plex behavior of the HCN abundance with expansion velocity is observed. There is a large dispersion in the values of HCN abundances for $V_e < 22$ kms^{-1}, with values that range from 10^{-7} to $> 10^{-4}$. Within this range of expansion velocities, if we select the stars with low mass loss rates studied by Olofsson et al. (1993) (asterisks in Fig. 6), the HCN abundance seems to decrease with expansion velocity. For velocities $V_e \geq 22$ kms^{-1}, the disperson is lower and values of about a few 10^{-5} are found for all the stars. If the stars with low mass loss rates are dropped, the HCN abundance seems to increase with expansion velocity. Jura (1991) and Olofsson et al. (1993) were studying different regions of this plot.

To understand the behavior of X(HCN) with V_e, it is very useful to represent the expansion velocity as a function of mass loss rate (see Fig. 7). For $\dot{M} \leq 2\ 10^{-6}$ $M_\odot$ yr^{-1}, the expansion velocity and $\dot{M}$ are well correlated. But for $\dot{M} > 2\ 10^{-6}$ $M_\odot$ yr^{-1}the curve is split into two branches. In one of them, the velocity is still correlated with $\dot{M}$ and V_e increases with $\dot{M}$ to values ~ 40 kms^{-1} (branch 1). The "high-V_e" stars belong to this branch. In the other branch, the expansion velocity remains constant to a value of about 15 kms^{-1} for $\dot{M}$ as large as 10^{-4} $M_\odot$ yr^{-1}(branch 2). Most of the best studied stars, like IRC+10126 and CIT 6, and the PPNe are included in this branch.

These two branches are responsible of the behavior observed when we represent X(HCN) against V_e. In the region of low expansion velocities ($V_e \leq 22$ kms^{-1}) we have the stars with low $\dot{M}$ and the stars with large $\dot{M}$ that belong to branch 2. The large dispersion of the X(HCN) values in this region is due mainly to an opacity effect. In this region, X(HCN) seems to decrease with increasing $\dot{M}$. In the region of high expansion velocities ($V_e >$ 22 kms^{-1}) we find the stars of branch 1. Since the opacity varies as $\tau \propto \dot{M}/V_e^2$, the envelopes of these stars are optically thinner than those of branch 2, and the obtained HCN abundances are not so seriously affected by opacity effects. Therefore, the high HCN abundances found toward the stars in branch 1 could be due, at least partially, to an opacity effect. These stars are those that appear as a small shoulder in Fig 5, and are those that we have called "high-V_e" stars.

To further investigate the possible dependence of the HCN abundance with the mass loss rate and the expansion velocity, we have represented X(HCN) against $\dot{M}/V_e^2$ (see Fig. 8). The values obtained for X(HCN) are surprisingly well correlated with $\dot{M}/V_e^2$. In this plot, there is no difference between stars with low and high expansion velocities. Does this dependence of X(HCN) on $\dot{M}/V_e^2$ have any physical meaning or is it just the consequence of a very optically thick emission in the HCN 1→0 line?. If the emission is very optically thick the brightness temperature depends very weakly on the parameters of the envelope. In this case, the HCN abundances calculated using expression (1) become strongly dependent on the factor $\dot{M}/V_e^2$. Using the radii and distances adopted for our calculations, expression (1) can be fitted by $X_{HCN} = 2.13\ 10^{-14}\ (\dot{M}/V_e^2)^{-1.3}\ T_{mb}$ for our sample of stars. In the optically thick limit, T_{mb} is expected to be quite uniform for all the stars, and $X_{HCN} \propto (\dot{M}/V_e^2)^{-1.3}$. The HCN abundances derived from our observations can be fitted by $X_{HCN} = 4.07\ 10^{-14}\ (\dot{M}/V_e^2)^{-1.1}$. Therefore, our values of the HCN abundance are consistent with the hypothesis of assuming a constant HCN abundance and very large opacities. We cannot conclude about the existence of any kind of variation of X(HCN) with $\dot{M}$, V_e or any other stellar parameter. The apparent variation of X(HCN) with these parameters are very likely due to an opacity effect. For comparison, we represent in Fig. 9 the C_2H abundance against $\dot{M}/V_e^2$. As it is easily seen from this plot, the abundance estimates are not correlated with $\dot{M}/V_e^2$ in this case in which the emission is not optically thick.

To determine accurate values of X(HCN), we have observed the $H^{13}CN$ J=1→0 line toward the "high-Ve" stars AFGL 809, IRC+00365, IRC+10401, IRC+30374, S Cep and AFGL 2901. The obtained abundances are X($H^{13}CN$) $\sim$ 0.8-7 10^{-6}, with $H^{12}CN/H^{13}CN$ ratios of 7-22. These ratios are larger than those obtained by Olofsson et al. (1993b) toward some prototypical C-rich stars. Assuming $H^{12}CN/H^{13}CN \sim 40$, we obtain that X(HCN)$\sim$ 3-30 10^{-5} in these stars (see Table 4). AFGL 809 and AFGL 2901 have HCN abundances $\approx 3\ 10^{-5}$ in agreement with the values obtained in the other C-rich stars, but IRC+00365, IRC+10401, IRC+30374 and S Cep have HCN abundances $> 10^{-4}$. These abundances are similar to those derived by Olofsson et al. (1993) toward stars with low $\dot{M}$ (and also low V_e). Olofsson et al. (1993) found values as large as $\sim 4\ 10^{-4}$ for some stars, but as they already discussed, values of X(HCN)$\gg 10^{-4}$ are very likely due to masering effects in the HCN 1→0 line. IRC+10216 is the best studied C-rich star. The most recent determination of the HCN abundance in IRC+10216 has been obtained by Cernicharo et al. (1996b) based on ISO observations. The obtained value, X(HCN)=3 10^{-5}, is much larger than the derived from the J=1→0 rotational line, but it is in agreement with the abundance estimated by Wiedemann et al. (1991) from the infrared spectrum. The large discrepancy between the values of the HCN abundance obtained from infrared and radio data, reinforce our hypothesis that the HCN J=1→0

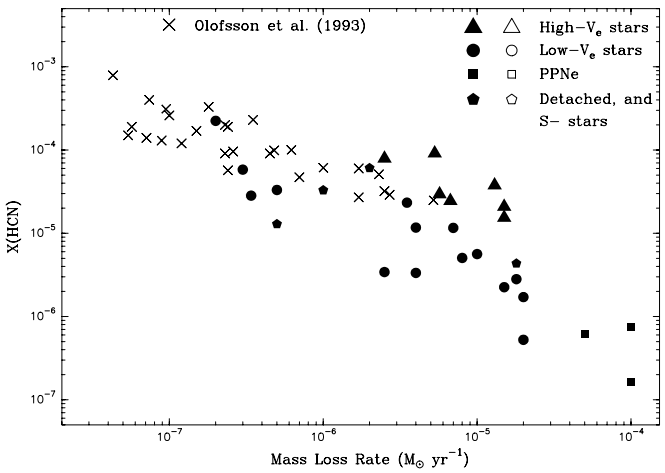

Fig. 5. HCN abundance estimates against the mass loss rate. Besides our data, we also show the abundance estimates reported by Olofsson et al. (1993) (asterisks). The other symbols are the same as in previous figures.

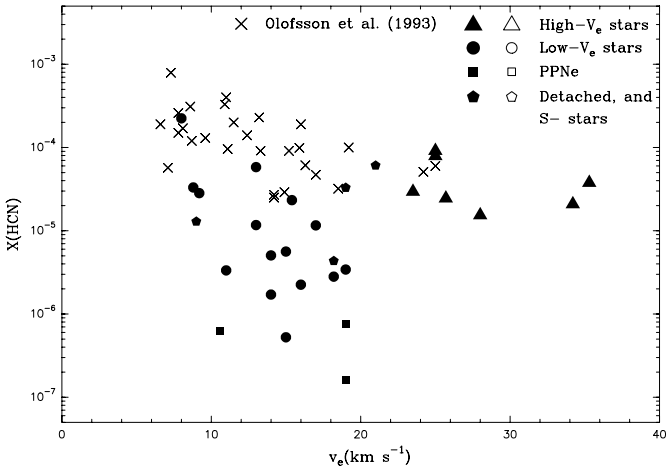

Fig. 6. HCN abundance estimates against the expansion velocity. The symbols are the same as in Fig. 5.

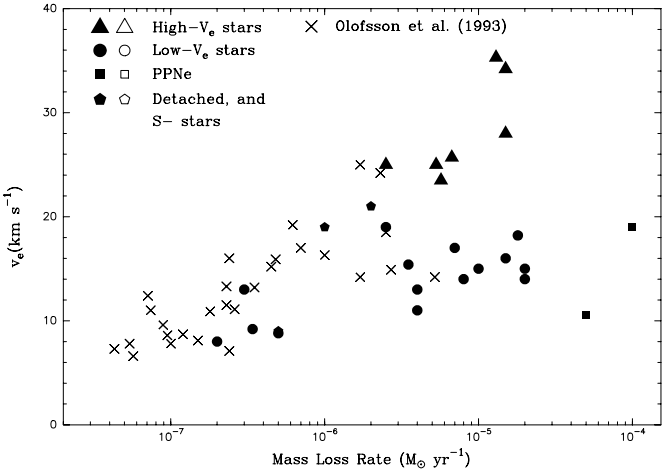

Fig. 7. Expansion velocity against mass loss rate. The symbols are the same as in Fig. 5.

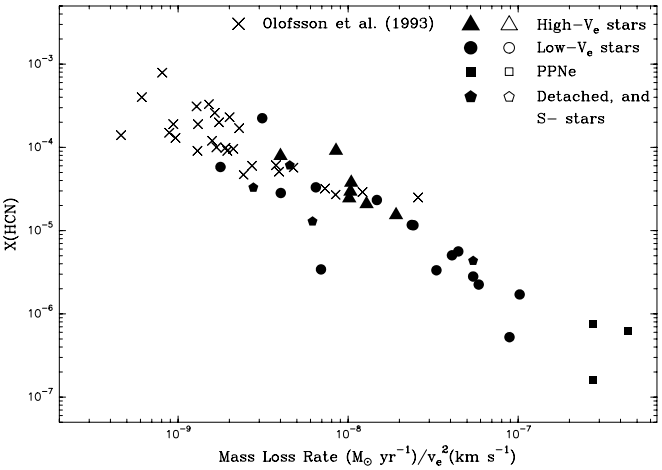

Fig. 8. HCN abundance estimates against $\dot{M}/V_e^2$. The symbols are the same as in Fig. 5.

line is very optically thick. Based on these results, we conclude that the HCN abundance is very likely $\sim$ a few 10^{-5} - 10^{-4} for all C-rich stars.

6. Discussion

6.1. C_2H: a photodissociation product of acetylene

The only way to estimate the C_2H_2 abundance in the outer envelope (at the photodissociation radius) is by inferring it from the observed C_2H abundance. Theoretical models by Cherchneff et al. (1993) and Millar & Herbst (1994) predict a C_2H/C_2H_2 peak abundance ratio of $\sim$ 0.3-0.5 depending on the C_2H_2 abundance. We have determined X(C_2H) = 1.0 10^{-5} toward IRC+10216. Assuming $C_2H/C_2H_2 \sim 0.4$, this would imply X(C_2H_2) $\sim$ 2.5 10^{-5} in this prototypical star. Based on infrared observations, Keady & Ridway (1993) estimated a C_2H_2 abundance of 8 10^{-5} toward IRC+10216, i.e., a factor of 3 larger than our estimate. A factor of 3 is within the uncertainties involved in abundance estimates. In spite of this, we would like to point out that from our C_2H observations we infer the C_2H_2 abundance at the photodissociation radius of C_2H_2, while the high excitation infrared lines trace mainly the C_2H_2 abundance in the accelerating gas of the inner envelope. Once the grains are formed, the refractory molecules of the outflowing gas, in particular C_2H_2, stick on their surfaces and their abundances could be significantly decreased at the photodissociation radius. This picture could also explain the variations found in the C_2H abundance with V_e in massive stars. We have obtained that the C_2H abundance, and consequently the C_2H_2 abundance at the photodissociation radius, is a factor of 5 larger in "high-V_e" than in "low-V_e" massive stars. The depletion of molecules onto grains as a function of the radius is given by,

$$\frac{dn_X}{dr} = -\pi a^2 n_X n f_g P V_D / V_e \qquad (2)$$

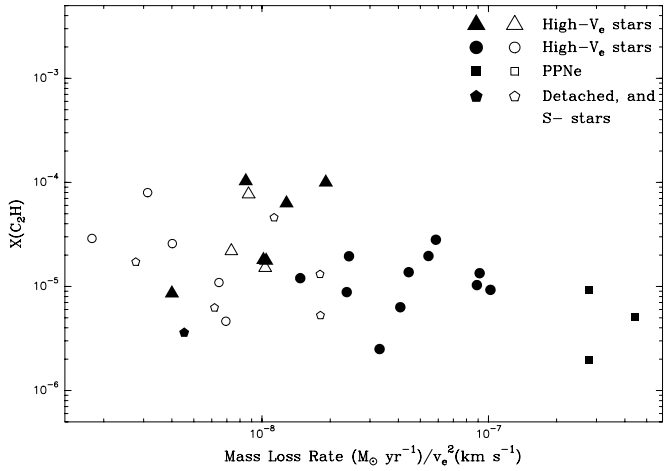

Fig. 9. C_2H abundance estimates against $\dot{M}/V_e^2$. Symbols are the same as in previous figures.

where n_X is the number density of the considered species, a is the radius of the grain, n is the hydrogen gas density, P is the sticking coefficient, f_g is the dust to gas ratio in number density ($f_g = n_g/n$ where n_g is the number of grains per volume unit), and V_D is the drift velocity of the dust grains to the gas. In a first approximation $V_D \propto V_e^{1/2}$. Assuming that once the grains are formed, the outflowing velocity remains constant through the envelope, and the gas density is given by $n = \dot{M}/(4\pi r^2 V_e)$, the depletion radius is $\propto V_e^{3/2}$. At the photodissociation radius, the C_2H_2 will be less depleted in a "high-V_e" than in a "low-V_e" massive star, and consequently, larger C_2H_2 abundances are expected in "high-V_e" stars.

We are aware of the simplicity of our model. In particular, it does not explain the different expansion velocities of the "low-V_e" and "high-V_e" massive stars. If the expansion velocity is produced by the radiation pressure on the grains, large expansion velocities are very likely related to a larger luminosity and/or to a higher dust opacity with respect to $\dot{N}$, i.e., mostly to a larger dust abundance. But this would also imply a higher depletion rate of C_2H_2 onto grains. On the other hand, C_2H_2 is thought to be an essential molecule in the formation of grains in C-rich envelopes. It is difficult to reconcile a larger dust abundance with a larger C_2H_2 abundance in the gas phase, unless one assumes a larger C_2H_2 abundance in the stellar photosphere. Furthermore, if one has a different dust content in "high-V_e" stars, the radius at which the grains are formed could also be different, and this would also change the depletion radius. In spite of these questions, our model can explain in a simple way the dependence of the C_2H_2 abundance with V_e in massive stars, and suggests some observational checks. If our model is correct, we should be able to detect a behavior similar to that of C_2H_2 in other compounds formed in the inner envelope like CS, SiS or SiO which should also be less depleted in "high-V_e" envelopes.

6.2. C_2H_2/HCN ratio

Although large uncertainties are involved in HCN abundance estimates, our results suggest that the HCN abundance ranges from $\sim 10^{-5}$-10^{-4} in all C-rich stars. Based on our C_2H data and the HCN abundance determined from ISO observations, we estimate a C_2H_2/HCN abundance ratio of $\sim$1 in IRC+10216. There are two groups of stars that seem to have X(HCN)$\sim 10^{-4}$, the stars with low $\dot{M}$ ($\dot{M} < 2\ 10^{-6}\ M_\odot\ yr^{-1}$), and the "high-$V_e$" stars ($\dot{M} \gtrsim 10^{-5}\ M_\odot\ yr^{-1}$ and $V_e \geq 22$ kms^{-1}). These two groups of stars have a very different behavior relative to the abundance of C_2H_2. While the stars with $\dot{M} \leq 2\ 10^{-6}$ $M_\odot\ yr^{-1}$ seem to be normal or slightly underabundant in C_2H (X(C_2H)$\leq 10^{-5}$), the mean C_2H abundance in "high-V_e" stars is a factor of 5 larger than in the other carbon stars. Based on our data, we estimate a C_2H_2/HCN ratio ≤ 0.1 in stars with low mass loss rates. A large dispersion in the values of the C_2H_2/HCN ratio is found in "high-V_e" stars. In S Cep we have obtained C_2H_2/HCN $\sim$0.08. This low value is due to the extraordinarily large abundance of HCN in S Cep. A large CN abundance is also found in S Cep (Bachiller et al. 1997). It is not clear whether S Cep is rich in nitrogenated compounds and/or these abundances are the consequence of the excitation of the HCN 1$\rightarrow$0 and CN 1$\rightarrow$0 lines. The C_2H_2/HCN ratio is $\sim$ 0.3, 0.45, 0.9 and 4 in IRC+30374, IRC+00365, IRC+10401, and AFGL 2901 respectively. These values are in agreement, within a factor of 4, with the value of the C_2H_2/HCN ratio in IRC+10126. AFGL809 is a special case. This star is overabundant in C_2H but has a low HCN abundance, and the C_2H_2/HCN ratio is 7. The data reported by Bachiller et al. (1997) show that the CN abundance is also low in this star. AFGL 809 seems to be deficient in nitrogenated molecules.

HCN abundances of 10^{-4} are an order of magnitude larger than the value predicted by thermodynamic models. HCN and N_2 are the most abundant nitrogen-bearing molecules in the photosphere of a carbon star. The HCN/N_2 abundance ratio is determined by the C/N ratio. A star rich in carbon is expected to have a large abundance of HCN but also a large abundance of C_2H_2 (see e.g. Tejero, 1991). In fact, the abundance of C_2H_2 is expected to be larger than the HCN abundance. Therefore, an enhanced C/N ratio can explain the results found in AFGL 809 and AFGL 2901, but it cannot account for the results on the stars with low $\dot{M}$ and the other "high-V_e" stars. To enhance the abundance of HCN without enhancing the abundance of C_2H_2 one has to invoke a nitrogen-rich envelope. An alternative explanation is that the large values of the HCN abundance observed toward low $\dot{M}$ stars and some "high-V_e" stars" are due to excitation effects. The excitation of C_2H and HCN could be strongly affected by infrared and optical pumping, specially in stars with low $\dot{M}$. Olofsson et al. (1993) suggested that the large HCN abundances observed toward low $\dot{M}$ stars could be due to masering effects in the HCN J = 1$\rightarrow$0 line. Bachiller et al. (1997) also suggested that excitation effects could produce the large CN abundances observed in low $\dot{M}$ stars. A detailed spectroscopic study of HCN and other nitrogenated molecules toward these stars is required to conclude about that.

7. Conclusions

We have observed a wide sample of C-rich stars in the C_2H and HCN millimeter lines using the 30-m IRAM telescope. Our results can be summarized as follows:

1. The mean value of the C_2H in "standard" C-rich stars is 2.5 10^{-5}. Lower values of the C_2H abundance ($X(C_2H) < 10^{-5}$) are found in S stars and stars with detached envelopes.
2. In "standard" C-rich stars, the C_2H abundance seem to be correlated with the expansion velocity. We have distinguished between "high-V_e" stars (stars with $V_e \geq 22$ kms^{-1}) and "low-V_e" stars (stars with $V_e < 22$ kms^{-1}). The abundance of C_2H in "high-V_e" stars is **a factor of 5 larger** than in "low-V_e" stars.
3. The mean acetylene abundance inferred from our observations is $\sim$ 3 10^{-5} in "low-V_e" stars and $\sim$ 1.2 10^{-4} in "high-V_e" stars.
4. The HCN abundance estimates derived from the HCN J=1$\rightarrow$0 rotational line are strongly affected by opacity effects. The apparent variations of the HCN abundance with V_e and $\dot{M}$ are very likely an opacity effect. This opacity effect is expected to be less important in stars with low mass-loss rates.
5. From $H^{13}CN$ observations, we have obtained that the HCN abundance ranges from 3 to 30 10^{-5} in "high-V_e" stars. These values are in the range of the HCN abundances found in "standard" C-rich stars. The most recent determination of the HCN abundance toward IRC+10216 is 3 10^{-5}. HCN abundances $\geq 10^{-4}$ are found by Olofsson et al. (1993) in stars with low-mass loss rates.
6. Large variations are found in the C_2H_2/HCN ratio. While a C_2H_2/HCN$\sim$1 is found toward IRC+10216, C_2H_2/HCN$\leq$0.1 in stars with low mass-loss rates, and values of C_2H_2/HCN$\sim$0.08-7 are found in "high-V_e" stars. Besides possible chemical differences between stars, excitation effects could also contribute to enhance the large dispersion of the observed C_2H_2/HCN ratios.

Acknowledgements. We are grateful to the technical staff of Pico de Veleta for their support during the observations. This work has been partially supported by the Spanish DGICYT under grant number PB93-0048.

References

Bachiller R., Fuente A., Bujarrabal V., Colomer F., Loup C., Omont A., de Jong T., 1997, A & A 319, 235
Bieging J.H., & Rieu 1988, ApJ 329, L107
Bujarrabal V., Fuente A., Omont A., 1994,A & A 285, 247
Cernicharo J., 1988, PhD. University of Paris VII
Cernicharo J., Guelin M., 1996a, A & A 309, L27
Cernicharo J., Barlow M.J., González-Alfonso E., et al., 1996b, A & A 315, 201.
Cherchneff I., Glassgold A.E., Mamon G.A., 1993, ApJ 410, 188
Heske A., Lintel Hekkert P.te, Maloney P.R., 1989, A & A 218, L5
Huggins P.J., Glassgold A.E., 1982, ApJ 252, 201
Jura M., 1991, ApJ 372, 208
Keady J.J., Ridgway S.T., 1993, ApJ 406, 199
Loup C., Forveille T., Omont A., Paul J.F., 1993, A & AS 99, 291
Lucas R., Guilloteau S, Omont A., 1988, A & A 194, 230
Millar T.J., Herbst E., 1994, A & A 288, 561
Nyman L.-Å., Olofsson H., Johansson L.E.B., Booth R.S., Carlström U., Wolstencroft R., 1993, A & A 269, 377
Olofsson H., Eriksson K., Gustafsson B., Carlström U., 1993, ApJS 87, 305.
Olofsson H., 1994, in "Molecules in the Stellar Environment", Proceedings IAU Colloquium 146, Jorgensen, U.G. (ed.), Springer Verlag.
Olofsson H., Bergman P., Eriksson K., Gustafsson B., 1996, A & A 311, 587
Omont A, 1992, "Millimeter observations and chemical processes in circumstellar envelopes and planetary nebular", Faraday Symposium Nº 28: Chemistry in the Interstellar Medium, Birmingham, 16-18 December 1992
Tejero J., 1991, in "Modelos de equilibrio termodinámico aplicados a envolturas circunestelares de estrellas evolucionadas", Instituto Geográfico Nacional (MOPT)
Truong-Bach, Nguyen-Q-Rieu, Omont A., Johansson L.E.B., 1987, A & A 176, 285
van Dishoeck EF. 1988, in "Rate Coefficients in Astrochemistry", eds.: TJ Millar & DA Williams. Dordrecht: Kluwer.
Wiedemann G.R., Hinkle K.H., Keady J.J., Deming D., Jennings D.E., 1991, ApJ 382, 321

This article was processed by the author using Springer-Verlag LaTeX A&A style file *L-AA* version 3.